Field-Induced Current Modulation in Nanoporous Semiconductor, Electron-Doped $12CaO \cdot 7Al_2O_3$

Toshio Kamiya,*[,†,‡] Shouzou Aiba,[†] Masashi Miyakawa,[§] Kenji Nomura,[‡] Satoru Matsuishi,[§] Katsuro Hayashi,[§] Kazushige Ueda,[†,||] Masahiro Hirano,[§] and Hideo Hosono[†,‡,§]

Materials and Structures Laboratory, ERATO-SORST, Japan Science and Technology Agency in Frontier Collaborative Research Center, and Frontier Collaborative Research Center, Tokyo Institute of Technology, 4259 Nagatsuta, Midori-ku, Yokohama 226-8503, Japan

Received August 24, 2005. Revised Manuscript Received September 27, 2005

$12CaO \cdot 7Al_2O_3$ (C12A7) has a unique crystal structure composed of positively charged cages ∼0.4 nm in inner diameter and a free oxygen ion (O^{2-}) clathrated in one-sixth of the cages. C12A7 can be converted to inorganic electride by replacing the clathrated oxygen ions with electrons, and the electride exhibits degenerate-type conduction with room-temperature conductivities >100 S cm^{-1}. In intermediate states, semiconductive C12A7 can be obtained by controlling electron density. In this study, we examined effects of electric field on carrier transport properties of the semiconductive C12A7 using a field-effect transistor (FET) structure targeted for future mesoscopic devices and electrochemical devices that will utilize the quantum-dot-like cage structures and chemically active clathrated anions in C12A7. FETs were fabricated using two types of samples, (i) single-crystalline bulk and (ii) polycrystalline thin films, for channels. First, conditions to form good contacts for source and drain electrodes were examined because the semiconductive C12A7 has a small work function, and it was difficult to form good electrical contacts with metals. It was found that Pt was the best metal with the lowest contact resistance to C12A7, and thermal annealing at ≥300 °C improved its non-ohmic characteristics. Electrical conductivity was modulated by 1−2 orders of magnitude by applying gate voltage. Apparent field-effect mobilities were 0.02−0.08 cm^2 $(V\ s)^{-1}$, which were comparable with the drift mobilities of the semiconductive C12A7. This is the first demonstration of a semiconductor device using an electride.

Introduction

Electrides are materials in which electrons behave like anions at a crystallographic periodic site.[1,2] As the electrons are bound loosely to the crystal, a variety of novel chemical and electronic properties, such as strong reducing power and excellent electron field emission, have been expected,[3] whereas, until 2003, all the electrides were synthesized using organic molecules and alkali metal elements and are not stable at room temperature (RT) or in an ambient atmosphere. This fatal drawback was overcome by employing a nanostructure in an inorganic crystal called C12A7 ($12CaO \cdot 7Al_2O_3$). The first RT-stable electride $[Ca_{24}Al_{28}O_{64}]^{4+}(4e^-)$ was fabricated from C12A7 by extracting oxygen ions accommodated in subnanometer-sized cages of C12A7 crystal selectively,[4] and efficient electron field emission was demonstrated at RT.[5]

Stoichiometric C12A7 is a typical electrical insulator with a fundamental band gap > 5 eV (taken from ref 6, but our recent data obtained on thin films indicate a larger value > 6 eV) and was not expected for an electronic active material. However, it has an exotic nanostructure embedded in the crystal structure by which C12A7 can be converted to a persistent electronic conductor. The crystal structure looks very complicated (Figure 1a), but it can be understood as follows: it has cages ∼0.4 nm in inner size (Figure 1b), and the closed packing of the cages forms the periodic crystal structure. As the cage framework is positively charged at $+4e$ (e is the elementary electric charge), stoichiometric C12A7 has two O^{2-} ions clathrated in 2 cages ("free oxygen ions") out of 12 cages in the unit cell. Therefore, new functions are rendered to C12A7 by replacing the free oxygen ions with active anions such as O^- (ref 7) and H^- (refs 8 and 9; clathrated anions). It is also possible to dope mobile electrons in the cages of C12A7 (clathrated electrons) by two methods: (i) introduction of H^- ions instead of the free oxygen ions (C12A7:H^-) followed by irradiation of utraviolet

* Corresponding author. E-mail: tkamiya@msl.titech.ac.jp.
† Materials and Structures Laboratory.
‡ ERATO-SORST, Japan Science and Technology Agency in Frontier Collaborative Research Center.
§ Frontier Collaborative Research Center.
|| Present address: Kyushu Institute of Technology, 1-1 Sensui, Kita-Kyushu 804-8550, Japan.

(1) Dye, J. L. *Inorg. Chem.* **1997**, *36*, 3817.
(2) Dye, J. L. *Science* **1990**, *247*, 663.
(3) Dye, J. L. *Science* **2003**, *301*, 607.
(4) Matsuishi, S.; Toda, Y.; Miyakawa, M.; Hayashi, K.; Kamiya, T.; Hirano, M.; Tanaka, I.; Hosono, H. *Science* **2003**, *301*, 626.
(5) Toda, Y.; Matsuishi, S.; Hayashi, K.; Ueda, K.; Kamiya, T.; Hirano, M.; Hosono, H. *Adv. Mater.* **2004**, *16*, 685.
(6) Watauchi, S.; Tanaka, I.; Hayashi, K.; Hirano, M.; Hosono, H. *J. Cryst. Growth* **2002**, *237*−*239*, 801.
(7) Hayashi, K.; Hirano, M.; Matsuishi, S.; Hosono, H. *J. Am. Chem. Soc.* **2002**, *124*, 738.
(8) Hayashi, K.; Matsuishi, S.; Kamiya, T.; Hirano, M.; Hosono, H. *Nature* **2002**, *419*, 462.
(9) Hayashi, K.; Toda, Y.; Kamiya, T.; Hirano, M.; Yamanaka, M.; Tanaka, I.; Yamamoto, T.; Hosono, H. *Appl. Phys. Lett.* **2005**, *86*, 022109.

10.1021/cm051904s CCC: $30.25
Published on Web 11/08/2005

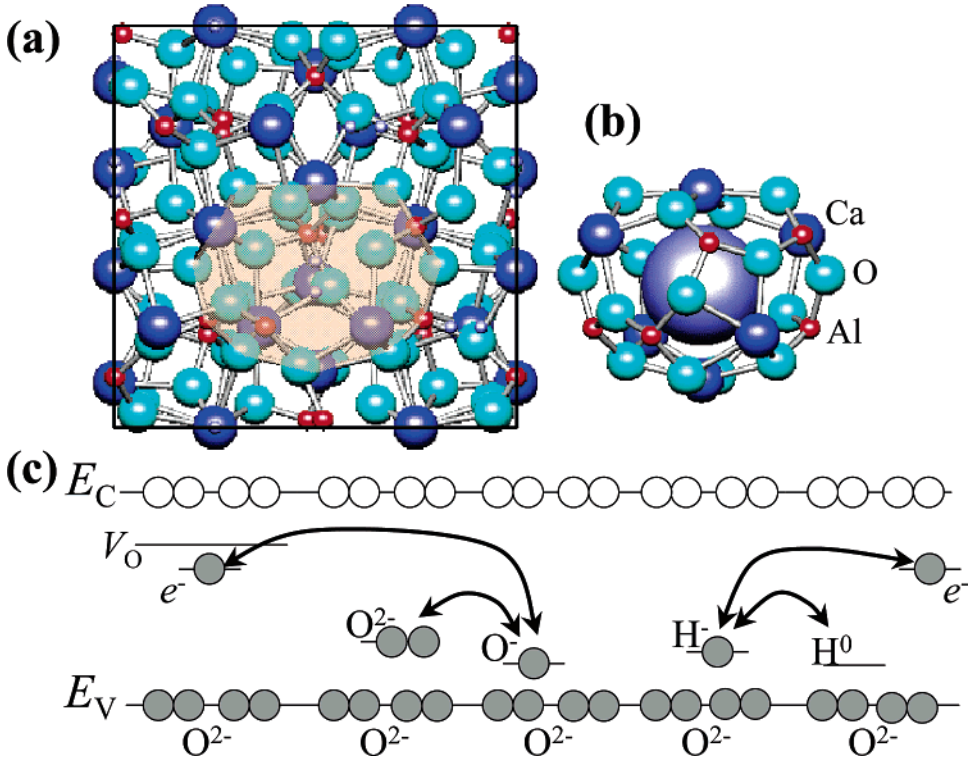

Figure 1. Crystal and electronic structures of C12A7-related materials. (a) Unit cell of stoichiometric C12A7. Clathrated ions are neglected for clarity. (b) Structure of a cage extracted from part a. The large sphere represents a clathrated anion. (c) Schematic electronic levels of clathrated anions. E_C, conduction band bottom, and E_V, valence band bottom of the cage framework of C12A7. V_O, electronic level of an empty cage, and e^-, that of an electron-clathrated cage. The electronic levels of the clathrate anions are formed in the fundamental band gap of C12A7. Charge transfer between the clathrated anions, which are induced by reactions O^{2-}(cage) + O_2(gas) ⇒ O^-(cage) + O_2^-(cage),[7,10] H^-(cage) ⇔ H^0(cage) + e^-(cage),[8] O^{2-}(cage) ⇒ $1/2O_2$ + $2e^-$(cage),[4] and so on, is the origin of emergence of new functions in C12A7.

(UV) light (C12A7:H^-:UV)[8] and (ii) removal of the free oxygen ions selectively from the cages (C12A7:e^-).[4] Thereby the electron concentration can be controlled from $<10^{17}$ to 2×10^{21} cm^{-3}. Thus, we may expect that the conductive C12A7 has potential as new exotic semiconductors.

As described above, charge transfer between the clathrated anions plays an essential role for the emergence of the active functions in the C12A7-derived materials.[10] Further, the cages of C12A7 can be regarded as coupled quantum dots,[11] and the electronic levels in the clathrated anions are largely changed by charge transfer so that they may work as a natural system of a charging island in a single-electron tunneling transistor.[12] Therefore, if it is possible to alter carrier generation or electronic potential in the cages of C12A7 by an external electric field as actually employed in conventional field-effect transistors (FETs), we may develop novel applications that can control the chemical activity, charged states of the clathrated anions, and electronic conduction. However, it is unclear whether such alternation of the carrier generation is possible in the semiconductive C12A7 or not, because the carrier transport mechanism and electronic structure of the semiconductive C12A7 are very different from the conventional semiconductors such as Si and GaAs.

It is reported that electron transport is controlled by hopping (i.e., small polaron) in the semiconductive C12A7,[13,14] which suggests that the electrons diffuse by repeating trapping at a localized state and thermal excitation from the trapping state to a neighboring trapping state. In addition, usually different anionic species such as O^{2-} and e^- coexist in C12A7, and they form electronic levels in the fundamental band gap of the cage framework as illustrated in Figure 1c.[12,13,15] From the general semiconductor physics, these levels might work as trapping states and pin the Fermi level. If this is the case in C12A7, the external electric field cannot alter the Fermi level: in other words, C12A7-based FETs cannot work. Therefore, it is of primary importance to explore field-induced phenomena in the semiconductive C12A7 before the above-mentioned mesoscopic applications are examined.

In this work, we have examined effects of external electric field on carrier transport properties of the semiconductive C12A7 using FET structures. Two types of semiconductive C12A7, (i) single-crystalline C12A7:e^- (sc-C12A7:e^-)[4] and (ii) UV-irradiated polycrystalline C12A7:H^- thin films (poly-C12A7:H^-:UV),[16] were employed for channels of FETs. First, we examined fabrication conditions of the semiconductive C12A7 applicable to FETs. Then, different electrode metals and thermal annealing were examined to form better

(10) Hayashi, K.; Matsuishi, S.; Hirano, M.; Hosono, H. *J. Phys. Chem. B* **2004**, *108*, 8920.
(11) Kamiya, T.; Hosono, H. *Jpn. J. Appl. Phys.* **2005**, *44*, 774.
(12) Kamiya, T.; Ohta, H.; Hiramatsu, H.; Hayashi, K.; Nomura, K.; Matsuishi, S.; Ueda, K.; Hirano, M.; Hosono, H. *Microelectron. Eng.* **2004**, *73*−*74*, 620.
(13) Sushko, P. V.; Shluger, A. L.; Hayashi, K.; Hirano, M.; Hosono, H. *Phys. Rev. Lett.* **2003**, *91*, 126401.
(14) Sushko, P. V.; Shluger, A. L.; Hayashi, K.; Hirano, M.; Hosono, H. *Thin Solid Films* **2003**, *445*, 161.
(15) Sushko, P. V.; Shluger, A. L.; Hayashi, K.; Hirano, M.; Hosono, H. *Appl. Phys. Lett.* **2005**, *86*, 092101.
(16) Miyakawa, M.; Hayashi, K.; Hirano, M.; Toda, Y.; Kamiya, T.; Hosono, H. *Adv. Mater.* **2003**, *15*, 1100.

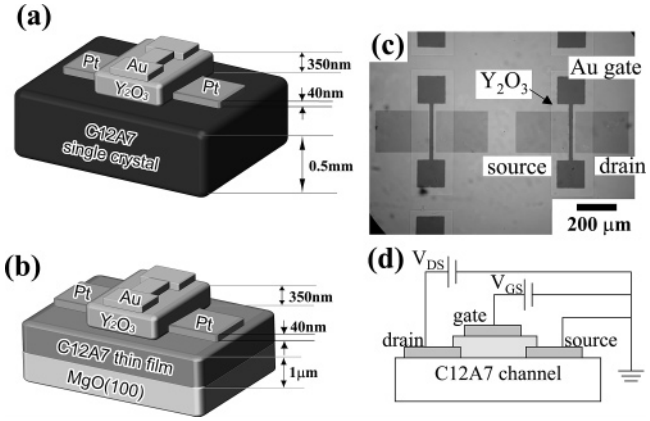

Figure 2. Device structures. (a) C12A7:e^- single-crystal channel and (b) polycrystalline C12A7:H^- thin film channel FETs. (c) Photograph of poly-C12A7:H^-:UV FETs. (d) Schematic illustration of the measurement circuit and notations of the applied voltages.

ohmic contacts for source and drain electrodes, because the semiconductive C12A7 has a small work function[5] and has difficulty forming an ohmic contact. Using the FETs, we confirmed that electrical current was modulated by 1−2 orders of magnitude by gate voltage if the appropriate electron concentration was chosen for the channel C12A7 materials.

Experimental Section

We examined two semiconductive C12A7: (i) sc-C12A7:e^- single-crystals and (ii) poly-C12A7:H^-:UV thin films. The C12A7:H^- films were fabricated by post-deposition annealing of amorphous C12A7 (a-C12A7) films and hot ion implantation of H_2^+.[16] First, 1-μm-thick a-C12A7 films were deposited by pulsed laser deposition (PLD) using an ArF excimer laser at a pulse energy of ~2.0 J cm^{-2} on MgO(100) substrates at RT under an oxygen pressure P_{O_2} of 3.0×10^{-3} Pa. The a-C12A7 films were then annealed at 1000 °C for 1 h in dry O_2 gas to produce poly-C12A7 films. Then, H_2^+ ions were implanted at 600 °C with an acceleration voltage of 120 keV. The fluence was varied from 10^{15} to 10^{18} cm^{-2}. The film thickness of ~1 μm was chosen from the projection length of H_2^+ ions calculated by a Monte Carlo simulation using a TRIM code.[17] Then UV light was irradiated to the poly-C12A7:H^- films (poly-C12A7:H^-:UV). Electron density was controlled by the total fluence of H_2^+ ions. The typical root-mean-square surface roughness of the films measured by atomic force microscopy was ~ 3.9 nm.

Sc-C12A7:e^- was prepared by the Ca-treatment method.[4] A 0.5-mm-thick C12A7 single-crystal plate[6] was sealed in a silica glass tube in a vacuum (~1 Pa) together with metal calcium shots and heated at 700 °C for durations varied from 4 to 240 h, which increased the electron density to a range from ~10^{17} to ~2×10^{21} cm^{-3}. The surfaces of the sc-C12A7 samples were mirror-polished with an Al_2O_3 polishing power of 1 μm in average size.

Top-gate, top-contact FET structures were fabricated using the semiconductive C12A7 for channels. (Figure 2a,b). The source, drain, gate contacts, and a gate insulator were defined by photolithography and lift-off techniques. Gate width and length were 300 and 50 μm, respectively. In preliminary experiments, we found that gate leakage current was rather high because of rather large roughness of the polycrystalline or mirror-polished surfaces of the channels. Therefore, we employed thick (~350 nm) gate insulators to suppress the leakage current. But a thick gate insulator reduced the gate capacitance and the carrier concentration inducible by gate voltage. Thus, we chose a gate insulator with a large dielectric constant (high-k dielectric), Y_2O_3, to keep a large gate capacitance with such a thick gate insulator. The Y_2O_3 layers were deposited by PLD at RT at a pulse energy of ~1.0 mJ·cm^{-2} and $P_{O_2} = 20$ Pa. The measured dielectric constant of the Y_2O_3 gate insulator was ~16ϵ_0 (ϵ_0 is the dielectric constant of a vacuum. That of the bulk Y_2O_3 crystal is ~16ϵ_0.)[18] Au was used for gate metal contact. For source and drain contacts, it was found that Pt formed better ohmic contacts with the semiconductive C12A7 channels among various metals, as will be discussed later. A photograph of a device chip is shown in Figure 2c. The electrical circuit used and the notation of the applied voltages (drain−source voltage V_{DS} and gate−source voltage V_{GS}) are illustrated in Figure 2d.

Optical absorption spectra were measured by a conventional spectrometer. Electron densities (N_e) were evaluated from integrated areas of the 2.8 eV optical absorption band induced in the semiconductive C12A7.[4,8] Electrical conductivity was extracted by alternating current impedance spectroscopy using a vector impedance analyzer (HP-4194A)[8] because it was difficult to form ohmic contact with the conductive C12A7. The metal electrodes were sputtered by an ion coater in Ar gas. FET characteristics were measured by semiconductor parameter analyzers (Agilent 4155C and Keithley SCS-4200).

Results and Discussion

First the relationship between fabrication condition and electronic properties of the semicodnuctive C12A7 was examined to find suitable conditions for fabricating FETs. Figure 3a shows optical absorption spectra of the sc-C12A7:e^-. The inset shows photographs of the samples. We can see that the Ca treatment induces two absorption bands at 0.4 and 2.8 eV, by which the sample color changes to green. We confirmed that the absorption band at 0.4 eV was due to intercage transition of a clathrated electron between neighboring cages and the 2.8 eV band was due to intracage transition and that the clathrated electrons contribute to electronic conduction as polaron.[13,14] Therefore, we assumed the density of mobile electrons (N_e) to be equal to that of the clathrated electrons evaluated from the integrated area of the 2.8 eV optical absorption band (denoted "F^+-like center" concentration, N_{F^+}, in refs 4 and 8). Similar absorptions were observed also in the poly-C12A7:H^-:UV films, and their electron densities were also evaluated by the same method.[16]

Figure 3b summarizes temperature dependences of electrical conductivities (σ) for various semiconductive C12A7. It is seen that the behavior of electrical conductivity is similar both in the sc-C12A7:e^- and in the poly-C12A7:H^-:UV, although drift mobilities (μ_{drift}) estimated from the σ and N_e values using the relation $\sigma = eN_e\mu_{drift}$ are almost 1 order of magnitude larger for the single crystals (e.g., $\mu_{drift} \sim 0.1$ cm^2 (V s)$^{-1}$ at $N_e \sim 10^{19}$ cm^{-3})[4] than that for the polycrystalline thin films (~0.03 cm^2 (V s)$^{-1}$;[16] Table 1), and this difference would be due to carrier scattering at the grain boundaries in the polycrystalline films. The σ shows the Arrhenius-type

(17) Ziegler, J. F.; Biersack, J. P.; Littmark, U. *The Stopping and Range of Ions in Solids*; Pergamon: New York, 1985.

(18) Kwo, J.; Hong, M.; Kortan, A. R.; Queeney, K. L.; Chabal, Y. J.; Opila, R. L.; Muller, D. A., Jr.; Chu, S. N. G.; Sapjeta, B. J.; Lay, T. S.; Mannaerts, J. P.; Boone, T.; Krautter, H. W.; Krajewski, J. J.; Sergnt, A. M.; Rosamilia, J. M. *J. Appl. Phys.* **2001**, *89*, 3920.

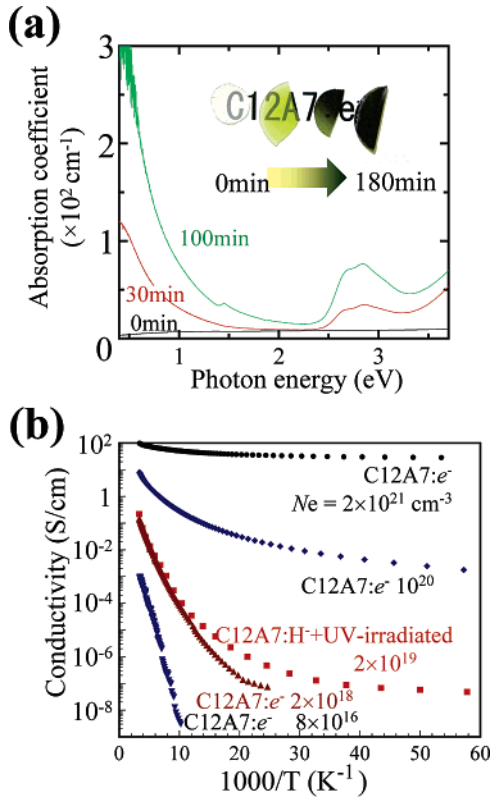

Figure 3. Optoelectronic properties of conductive C12A7. (a) Optical absorption spectra of sc-C12A7:e^- Ca-treated for 0, 30, and 100 min. Similar absorption spectra were observed for poly-C12A7:H^-:UV thin films. (b) Temperature dependence of electrical conductivity for sc-C12A7:e^- and poly-C12A7:H^-:UV thin films. Increase in electrical conductivity is accompanied by green coloration (inset to part a) and the appearance of two absorption bands at 0.4 and 2.8 eV (a).

Table 1. Electronic Properties and FET Parameters of Conductive C12A7 Examined[a]

	C12A7:e^-	C12A7:e^-	C12A7:e^-	C12A7:H^-
conductivity (S cm^{-1})	4×10^{-3}	2×10^{-1}	1	~0.1
carrier concentration, N_e (cm^{-3})	~5×10^{17}	~10^{19}	~10^{20}	~2×10^{19}
apparent field-effect mobility, μ_{ap} [cm^2 (V s)$^{-1}$]	0.01	0.08		0.02
on/off current ratio	~10	~10		~100
drift mobility, μ_{drift} [cm^2 (V s)$^{-1}$]	~0.05	~0.1		~0.03

[a] The drift mobility (μ_{drift}) values were estimated from data in refs 8 and 16.

thermal activation behavior if the RT conductivity is lower than 10^{-3} S cm^{-1}, while it exhibits deviation from the Arrhenius type behavior for higher conductivity samples, especially at low temperatures. In the latter case, the logarithm of the conductivity follows well the −1/4 power law in an intermediate conductivity range, suggesting that the electrons run through distribution of potential barriers in the semiconductive C12A7 and effective activation energy changes with temperature.[4,19] When the conductivity reaches the maximum value ~100 S cm^{-1}, it shows very small variation against temperature so as that conduction mechanism may be regarded as almost degenerated conduction.

For FET applications, we should notice that the carrier concentration in a channel of a FET must be controlled to well below 10^{17} cm^{-3} because typical carrier density controllable by external electric field is as high as the order of 10^{18} cm^{-3} in a usual FET structure. This requirement suggests conductivity should be controlled to a value lower than 10^{-3} S cm^{-1} for the sc-C12A7:e^- and 10^{-2} S cm^{-1} for poly-C12A7:H^-:UV films (estimated using the μ_{drift} values above). However, this estimation turned out not to work well, and, therefore, we surveyed the channel materials in a wider range of N_e (the reason will be discussed later). The typical samples examined are listed in Table 1, which include (i) sc-C12A7:e^- with conductivities ~4×10^{-3} ($N_e \sim 5 \times 10^{17}$ cm^{-3}), 2×10^{-1} ($N_e \sim 10^{19}$ cm^{-3}), and ~1 S cm^{-1} ($N_e \sim 10^{20}$ cm^{-3}) and (ii) poly-C12A7:H^-:UV films fabricated with H_2^+ implanted at 5×10^{16} cm^{-2} that have a conductivity of ~0.1 S cm^{-1} and $N_e \sim 2 \times 10^{19}$ cm^{-3}.

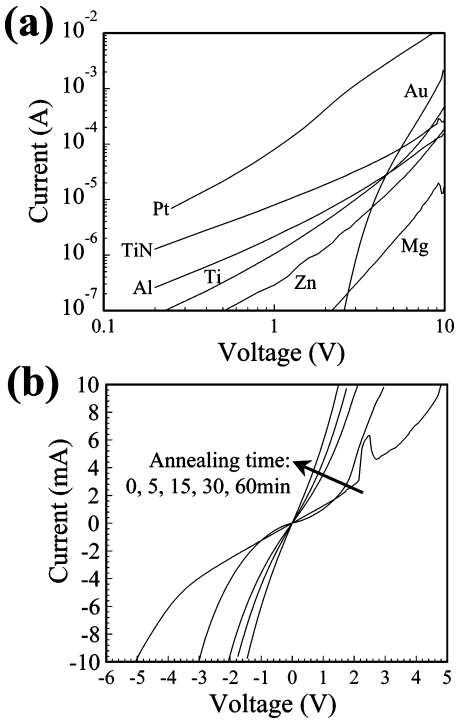

Figure 4. $I-V$ characteristics measured using a two-probe configuration at RT. (a) $I-V$ characteristics of sc-C12A7:e^- using various metal electrodes. (b) $I-V$ characteristics of sc-C12A7:e^- annealed at 500 °C for various durations. Pt was used for the electrodes.

Another issue to be considered for FETs is source−channel and drain−channel contacts. Because the conductive C12A7 has a small work function (~3.7 eV was obtained for the largest conductivity sc-C12A7:e^- by UV photoelectron emission),[5] it is difficult to form good ohmic contact with metals. Figure 4a shows current−voltage ($I-V$) characteristics of the sc-C12A7:e^- having various metal contacts measured at RT. These characteristics were measured using a two-probe configuration and, therefore, were affected strongly by the non-ohmic metal contacts. It is seen that all the metal contacts show strong nonlinearity, indicating the formation of Schottky barriers (see the slopes in the log−log plot, which should be unity for an ohmic contact). Among them, we chose Pt because it has the lowest contact resistance. It was found that the Pt contact was dramatically improved by thermal annealing in a vacuum at ≥300 °C. Figure 4b shows $I-V$ characteristics of the sc-C12A7:e^- with Pt contacts annealed at 500 °C as a function of annealing

(19) Nomura, K.; Ohta, H.; Ueda, K.; Kamiya, T.; Hirano, M.; Hosono, H. *Appl. Phys. Lett.* **2004**, *85*, 1993.

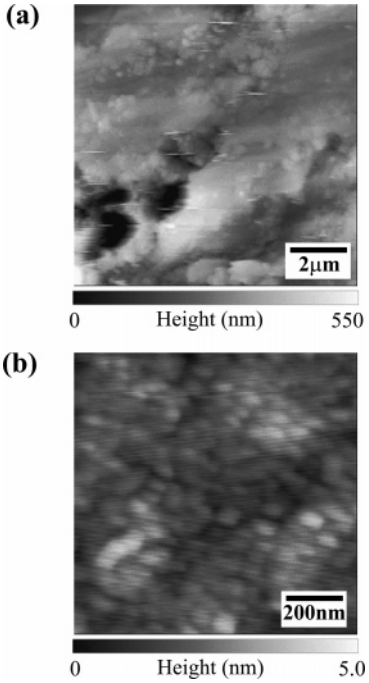

Figure 5. Atomic force microscopy images of (a) sc-C12A7:e^- and (b) poly-C12A7:H^- after ion implantation. The root-mean-square surface roughness of the poly-C12A7:H^- film was 3.9 nm

time. We speculate that the shallow surface region of the sc-C12A7:e^- was slightly oxidized before annealing because the samples were exposed to air after the Ca treatment. It may form rather high Schottky contact with metals. When it was annealed at ≥300 °C, the excess surface oxygen would diffuse into the deeper bulk region and increase electron density near the metal−C12A7 interface, improving the electrical property of the metal contacts. Thus, we employed thermal annealing of sc-C12A7:e^-/Pt samples at 500 °C for 60 min before fabricating FETs. However, this technique cannot be used for poly-C12A7:H^-:UV because the conductive state induced by UV irradiation is recovered to the initial insulating state by heating at ≥300 °C.[8]

Then, we fabricated top-gate, top-contact FETs using the sc-C12A7:e^- (Figure 2a) and the poly-C12A7:H^-:UV (Figure 2b) for channels. When the gate insulator structure was optimized, we found that rather thick gate insulators were necessary to suppress gate leakage current, because the surfaces of both the mirror-polished sc-C12A7:e^- and poly-C12A7:H^-:UV had somewhat large surface roughnesses (Figure 5a,b). Therefore, we employed the large gate insulator thickness of ∼350 nm. To keep a large gate capacitance for this large thickness, we needed to choose a gate insulator having a large dielectric constant (high-k dielectric). After several high-k dielectrics were screened, we employed Y_2O_3 for the gate insulator.

Figure 6a,b shows FET characteristics of the sc-C12A7:e^- FET. The sc-C12A7:e^- had the N_e value of $\sim 10^{19}$ cm^{-3}. The drain−source current I_{DS} markedly increases as drain−source voltage V_{DS} increases at a positive gate bias (V_{GS}), indicating that the channel is n-type. The I_{DS} exceeds 10 μA at V_{DS} of 25 V and V_{GS} of 16 V. Unlike usual FETs, it does not exhibit pinch-off, and the output characteristic is highly nonlinear, suggesting that the drain−source current is still limited by non-ohmic Pt−channel contacts. The on−off current ratio is about 10. This value is low but clearly shows that carrier generation is controlled by the gate voltage.

As the FET characteristics do not follow the standard simple FET theory and the channel layer is very thick (0.5 mm), it is difficult to evaluate a field-effect mobility having valid physical meaning. Nevertheless, such estimation would still provide an indication of the quality of the device and the channel material. Here, we evaluated apparent field-effect mobilities (μ_{ap}) from the largest slope of the output $I_{DS} - V_{DS}$ characteristics using the differential of the standard equation $I_{DS} = (\mu_{ap} C_i W/2L)[V_{GS} - V_T - (V_{DS}/2)]V_{DS}$, where C_i, W, L, and V_T denote the gate capacitance, channel width, channel length, and threshold gate voltage, respectively. The estimated μ_{ap} value is ∼0.08 cm^2 (V s)$^{-1}$ for the sc-C12A7:e^- FET with $N_e \sim 10^{19}$ cm^{-3}. It shows reasonable consistency with the drift mobility of sc-C12A7:e^-, $\mu_{drift} \sim 0.1$ cm^2 (V s)$^{-1}$. For the sc-C12A7:e^- FET with $N_e \sim 5 \times 10^{17}$ cm^{-3}, lower μ_{ap} values ∼ 0.01 cm^2 (V s)$^{-1}$ were obtained (Table 1). It would be partly explained by the fact that drift mobility of sc-C12A7:e^- increases with the electron density (Table 1), which is caused by the hopping polaron conduction. In addition, as the gate electrodes did not cover the whole region of the channel to suppress gate leakage current as seen in Figure 2c,d, the residual parts of the channel remained resistive and caused the lower μ_{ap} values for the FET with the lower conductivity channel. When the most conductive C12A7:e^- ($N_e \sim 2 \times 10^{21}$ cm^{-3}) was used for a channel, the FET did not work, which is reasonable because the carrier concentration in the channel is too large to be altered by the gate voltage.

The characteristics of the poly-C12A7:H^-:UV thin film FET (Figure 6c,d) look similar to those of the sc-C12A7:e^- FET. A relevant difference is the on current, which is almost 2 orders of magnitude lower (∼0.25 μA) than that obtained in the sc-C12A7:e^- FET. It comes partly from the lower V_{GS}, which was limited by gate leakage in this case. The μ_{ap} value was estimated to be ∼0.02 cm^2 (V s)$^{-1}$, which is approximately 1 order of magnitude smaller than that of the sc-C12A7:e^- FET and is also responsible for the small on current. However, this value is almost consistent with the drift mobility of the poly-C12A7:H^-:UV films. Hysteresis was also measured on the poly-C12A7:H^-:UV FET, showing small negative voltage shifts <1 V. The on−off current ratio is improved to ∼100 from that of the sc-C12A7:e^- FETs. It would be because the drain−source leakage current occurs in the deep region of the thick channel substrates in the sc-C12A7:e^- FETs, while it is suppressed by employing the thin channel layer in the poly-C12A7:H^-:UV thin film FET. However, the poly-C12A7:H^-:UV channel is still very thick (∼1 μm) for usual FETs (typically ≪ 100 nm), which would still cause the drain−source leakage current in the off state.

Finally, we like to discuss the electron density in the channel materials. In the present case, the sc-C12A7:e^- and poly-C12A7:H^-:UV worked as the channels of the FETs even though they have large electron concentrations ≥10^{19} cm^{-3} in the as-prepared states (i.e., before fabricating the FETs). It would be plausible that the electron concentration was reduced in the fabrication processes of the FETs. We needed to use a high oxygen pressure of 20 Pa to form the

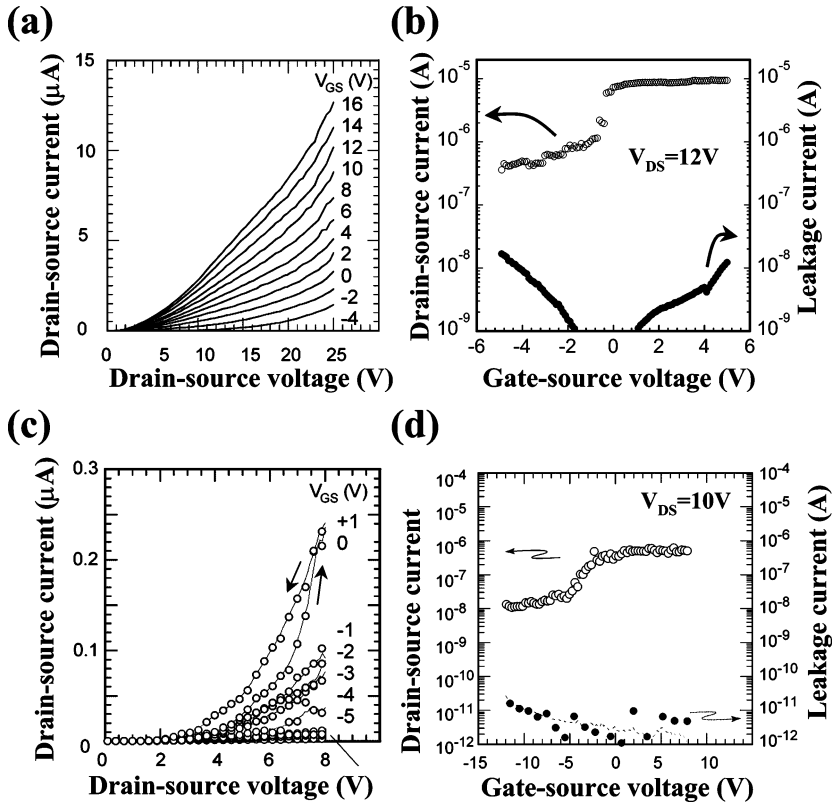

Figure 6. Characteristics of C12A7-based FETs measured at RT. (a, b) Output and transfer characteristics of sc-C12A7:e^- FET and (c, d) those of poly-C12A7:H^-:UV thin film FET.

Y_2O_3 gate insulator to suppress gate leakage current. Also, our photolithography patterning process used water-based solutions. These processes would oxidize the channel surface partially and reduce actual electron concentrations in the channels. Although the operation of the FETs was confirmed with several chips fabricated by different processing runs, it should be noted that the present yield rate of these FETs is not good (5 chips out of more than 30 chips worked), probably as a result of the sensitivity and difficulty in our device process and the difficulty in suppressing the gate leakage described above.

Conclusions

We demonstrated operation of the FETs using the C12A7-derived semiconductors as channels. This is the first demonstration of a semiconductor device using an electride. The performance of the FETs may be improved by finding better source and drain contacts and forming much smoother surfaces of the channels to suppress gate leak and to reduce the thickness of the gate insulator. The present results clarified that the carrier generation in the C12A7-derived materials can be controlled by external electric fields. In other words, the other clathrated anionic species do not control the field-induced phenomena in the present case. It would be because few active radicals such as O^-, which might work as electron traps, were formed by the fabrication condition used in this study. It would be also possible to control the charged states of the clathrated chemical species if active radicals are selectively introduced in the C12A7 channel by choosing appropriate fabrication conditions.

Acknowledgment. This work was supported in part by the Grant-in-Aid for Scientific Researches (Creative Research, No. 16GS0205) from the MEXT, Japan.

CM051904S